5-2012

Streambed Thermal Property Instrument SPI

James Alwel Dayie
Utah State University

STREAMBED THERMAL PROPERTY INSTRUMENT (SPI)

by

James Alwel Dayie

A report submitted in partial fulfillment
of the requirements for the degree

of

MASTER OF SCIENCE

in

Mechanical Engineering

Approved:

……..	……..
Dr. Heng Ban	Dr. Byard Wood
Major Professor	Committee Member

……..
Dr. Wenbin Yu
Committee Member

UTAH STATE UNIVERSITY
Logan, UT

2012

ABSTRACT

Streambed Thermal Property Instrument

by

James Alwel Dayie, Master of Science

Utah State University, 2012

Major Professor: Dr. Heng Ban
Department: Mechanical and Aerospace Engineering

The purpose of this research, the Streambed thermal Property Instrument (SPI) is to determine the applicability of this instrument for in situ thermal (conductivity and diffusivity) and porous flow (magnitude and direction) measurements. Currently, no such thermal instrument exists for such in situ measurements and the reason for developing this unique instrument, the SPI to fill the technology gap in sediment thermal property measurement devices. Prior to testing the instrument under controlled laboratory conditions to determine its functionality through a series of static and flow tests, the instrument was designed and built. A lab-sized version of an actual river called a flow cell with a gravity-driven flow was also built, making it possible for testing the SPI under controlled lab conditions .The instrument was tested in the flow case by fixing the instrument in two orientations in the saturated porous media (glass particles). Results from the static tests indicated that these bulk thermal measurements (diffusivity and conductivity) can be off the expected value by as much as 15% while the porous flow measurements (magnitude and direction) displayed more variability in results for the two orientations of the probe for the flow rate range considered. This variability in flow measurements has been partly attributed to the movement of the offset probes during insertion and rotation and the large size of the center probe of the SPI. The findings from this research has made it possible for more advanced research in this field by using computer simulations to make possible, accurate porous flow measurements using a large scale thermal probe such as the SPI.

(45 pages)

Key words: *Porous Media (Glass beads), Bulk Thermal Conductivity, Bulk Thermal Diffusivity, Porous Flow, Streambed Thermal Property Instrument.*

ACKNOWLEDGMENTS

My first and foremost gratitude goes to my major professor, Dr. Heng Ban who has been very helpful with his knowledge and expertise in thermal property measurement and porous media flow.

Secondly, I am also grateful to Dr. Byard Wood and Dr. Wenbin Yu and again my major professor for serving on my committee despite their very busy schedules and reading through this report and giving me suggestions towards making this report a better one.

I am heartily thankful to my fellow researcher, Eli Wilson for his encouragement, guidance and support through every step of the way that has helped me to develop a deeper understanding of the research from the very day I took up on this research project until now. He also gave me very good suggestion towards writing this report and made vital corrections to it as well.

My appreciation also goes out to Daniel Garrett who made very detailed corrections to the language and grammar and also gave me some very good suggestions towards making this report a really good one.

I offer my regard and blessings to the rest of Dr. Ban's research team for their suggestions and support during our weekly group meetings.

Last but not the least, I am very grateful to my parents whose financial support, prayers and regular advice have been beyond measure during this endurable journey, I say I am forever grateful for whatever they have invested in me.

James Alwel Dayie

CONTENT

Page

LIST OF TABLES

Table Page

LIST OF FIGURES

ACRONYMS

SPI	Streambed thermal Property Instrument
Flow_SV	Flow solver for fixed radius
TC	Thermocouple
OC	Off-Center
P	Probe

NOMENCLATURE

T	Temperature, [K]
V_x	Thermal advection velocity component in the x-direction, [ms^{-1}]
V_y	Thermal advection velocity component in the y-direction, [ms^{-1}]
V	Absolute value of the heat velocity, [ms^{-1}]
φ	Angle of flow with respect to the x-direction, [degrees]
J_x	Water flux in the x-direction, [ms^{-1}]
J_y	Water flux in the y-direction, [ms^{-1}]
C_w	Volumetric heat capacity of water, [$Jm^{-3}K^{-1}$]
C	Volumetric heat capacity of the system, [$Jm^{-3}K^{-1}$]
x'	New coordinate value of x after rotation through angle, φ[m]
y'	New coordinate value of y after rotation through angle, φ[m]
t_o	Finite time of heat supply, [s]
λ	Thermal conductivity of the porous media, [$Wm^{-1}K^{-1}$]
q'	Heat input per unit length per unit time, [Wm^{-1}]
κ	Thermal diffusivity, [$m^2 s^{-1}$]
r	Spacing between the heater (center) and offset probes(temperature sensors),[m]

CHAPTER 1

INTRODUCTION

Thermal properties of soil and porous flow measurements are essential for acquiring in-depth knowledge of water and heat transport phenomena in the vadose or unsaturated zone, determining infiltration rates, surface run-off and subsurface processes and also in engineering applications where temperatures and water fluxes are of prime interest. Temperature is an important component of aquatic systems due to its integral relationship with biological and chemical reaction rates. Current stream temperature models available to assist in managing heat load allocations are quite limited in their range of applicability as they do not include the effect of bed conduction, dead zone (surface) and the hyporheic zone (subsurface) storage. Apart from needing to characterize the soil's physical properties, i.e. soil thermal conductivity and soil thermal diffusivity, knowledge of the soil thermal properties is required for accurate prediction of soil temperature and its influence on seed emergence and crop growth, soil water retention and unsaturated hydraulic, and soil water vapor flow in coupled water and heat transport.

Earlier research findings prior to the development of the Streambed Thermal Property Instrument (SPI) have shown promising abilities of measuring bulk thermal properties and water flux of saturated porous media [7][8][9]. However, currently there exists no such instrument for accurately quantifying bulk streambed thermal properties and hence the need for the development of a modern day device to fill the technology gap in sediment thermal property measurement devices.

The SPI, which has already been built and tested under controlled lab conditions, will be used for *in situ* measurement of bulk thermal properties of saturated streambeds as well as measurement of porous flow through the streambed. Determination of water movement in porous media is critical for managing irrigation and drainage and characterizing chemical transport

processes. The instrument was designed with two Utah rivers in mind, namely Curtis Creek, east of Hyrum, UT, and the Virgin River in Hurricane, UT.

The SPI measures the streambed's bulk thermal conductivity and bulk thermal diffusivity as well as the porous flow magnitude and direction of flow through the streambed. The SPI has considerably improved upon conventional methods of measuring these thermal properties by eliminating the need to remove soil samples from the streambed for laboratory processing to obtain desired results. This ensures a much faster and a more accurate means of measuring bulk thermal properties and porous flow parameters. Adding to the improvements that the SPI has brought to the field of sediment thermal measurements, it is more cost effective and also less labor-intensive to make these thermal measurements compared to the conventional method. It is an improvement upon the current and previous time consuming, mathematically complicated and the measurement-intensive approaches of measuring these quantities.

CHAPTER 2

OBJECTIVES

The objectives of this research were to:

- design
- build and
- determine the functionality of the SPI through a series of bench tests under controlled laboratory conditions.

Testing the instrument at environmentally controlled conditions will yield the instrument's range of applicability from the measurement errors obtained. The consistency of these errors allow for calibration of the instrument for actual field testing.

Determining the functionality of the instrument was achieved by conducting laboratory experiments using yellow sand (glass particles) as the porous media over a wide range of flow rates. Static tests were conducted to determine the bulk thermal conductivity and bulk thermal diffusivity of the porous media. Flow tests were also run while keeping the instrument in two orientations (90° and 120°) to measure the porous flow. The flow through the flow cell containing the porous media was gravity-driven.

CHAPTER 3

LITERATURE REVIEW

Transient methods of thermal property measurement have been gaining popularity over steady-state methods because transient methods require much less time to perform. It is very challenging to determine steady state conditions in fluids because of the occurrence of natural convection. Consequently, it is difficult to eliminate the effect of natural convection on heat flux. One particular method is the hot-wire method, which is quick, mathematically convenient, most accurate, reliable and above all a very robust technique (Hammerschmidt & Sabuga [10]), for evaluating the thermal conductivity of fluids (de Groot, Kestin and Sookiazian [11], Healy, de Groot and Kestin [12], Kestin and Wakeham [13]) and solids (Assael *et al*. [14]). The Hot Wire Method relies on a simple analytical formula derived from the solution of the heat conduction from a line heat source that is inserted into the saturated porous media of interest. Application of this method works very well with gases and solids, however, applying this method to electrically conducting liquids requires further research. Limitations of the method have been identified and discussed by Valdasz [15]. He concluded that it is incorrect to apply the method directly to two-phase systems without corrections. The hot-wire method uses a wire to heat a fluid, and the thermal conductivity of the fluid or whatever sample is being heated by the wire may be derived from the wire's temperature response.

An adaption of the hot-wire method is the thermal probe as outlined in ASTM standard D5334 [1]. The thermal probe causes minimal intrusion and is easily inserted into saturated porous media and even into solids. The thermal probe is capable of measuring the effective (bulk) thermal conductivity. Commercial probes are available such as Decagon Device's KD2 series of probes capable of measuring bulk thermal conductivity, bulk thermal diffusivity, specific heat and thermal resistivity using the transient line heat source method.

By adding off-center probes around a thermal probe, the instrument is able to measure the effective (bulk) thermal diffusivity of the media. This concept is also found commercially in Decagon Device's specialized dual needle probe (KD2-Pro). Research at Utah State University was done using a thermal probe with four off-set probes called a penta-probe [2]. The penta-probe was inserted into porous media and measured the bulk thermal properties as well as the porous flow magnitude and direction by using a pulse heat signal. The SPI is essentially a large-scale version of the penta-probe.

Increasing the scale of the probe is not a trivial task. Large scale probes cannot fit the infinitely-thin assumption made by both the hot-wire method and thin thermal probes. Multiple designs of large thermal probes have been researched, and the probe's diameter and composition affect the thermal response, particularly during the initial heating time [3]. Large probes require correction factors, due to their distinction from the theory. The correction factors are functions of the construction of the probe. With proper correction factors selected, large thermal probes may effectively measure bulk thermal conductivity. Attempts have been made to liken a large probe to a composite cylinder [4] allowing for a mathematical model of the thermal response. However such methods are less popular than the correction factor approach.

Designs have varied over the years, but generally follow de Vries and Peck's [5] advice for creating a cylindrical probe: the probe should have a low volumetric heat capacity compared to the media, and the thermal conductivity of the probe should be larger than the material. Barrie W. Jones [6] gave insight into the valid time responses of larger probes.

Further complications arise when large probes are used in conjunction with off-set probes for bulk thermal diffusivity measurement. Conductivity escapes these complications by being largely a function of the probe's temperature response after a long heating time. The initial heating in a large-diameter probe is vastly different from one which fits an infinitely thin

assumption due to the probe's heat capacitance. For this reason, pulsed heating is not appropriate for large probe. The bulk thermal diffusivity measurement is largely a function of the probe response during the initial heating. For accurate diffusivity measurements, the ratio of the probe's thermal diffusivity to the bulk media's diffusivity must be converted into an effective thermal radius. With proper adjustment, a large thermal probe may be used with off-set probes for accurate bulk thermal diffusivity measurement.

Finally, a large thermal probe greatly affects the flow measurement. This is due to the large probe's obstruction of the flow path. Flow slows down immediately upstream and downstream the probe, causing greater increase in temperature in these regions. Similarly, flow speeds up as it moves around the probe, causing smaller temperature increase in regions normal to the flow vector. These changes in temperature response result in a skewed measurement of flow magnitude and direction. The disrupted flow path must be taken into account.

Flow through a porous media was first fitted to an equation conforming to Darcy's Law:

$$\nabla^2 P = 0 \tag{1}$$

His law may be applied to give a flow vector field around a circular cylinder. Such a vector field accurately describes the flow around a large diameter probe.

CHAPTER 4

THEORY

The theory of a SPI probe is taken from the heating portion of the penta-probe. The equation for combined heat conduction and convection in a two dimensional domain for uniform transport of water in an incompressible porous medium assuming an infinitely thin center probe and also that for conductive heat transfer dominant over convective effects is given by [14]. The heat equation (2) below assumes that at any point in the solid-fluid porous matrix the two temperatures are identical [15],

$$\frac{\partial T}{\partial t} = k\left(\frac{\partial^2 T}{\partial x^2} + \frac{\partial^2 T}{\partial y^2}\right) - V_x\frac{\partial T}{\partial x} - V_y\frac{\partial T}{\partial y} \tag{2}$$

where T is the temperature in Kelvin (K), k is the bulk thermal diffusivity of the system (m^2/s), V_x and V_y are the components of the thermal advection velocity, defined as:

$$V_x = \|V\|\cos\varphi \quad \text{and} \quad V_y = \|V\|\sin\varphi \tag{3}$$

where φ is the angle of flow with respect to the x-direction as seen below in Fig. 1.

The thermal advection velocity can be related to the water flux according to the equations below.

$$V_x = J_x\frac{C_w}{C}, \qquad V_y = J_y\frac{C_w}{C} \tag{4}$$

where J_x and J_y are the water fluxes (m/s) in the x and y directions respectively, C is bulk volumetric heat capacity ($Jm^{-3}K^{-1}$]) of the system, C_w is volumetric heat capacity of water.

The analytical solution for Eq. 2 may be obtained by coordinate rotation to align so the x'-direction with the water flow direction by applying the following transformation,

$$\begin{pmatrix} x' \\ y' \end{pmatrix} = \begin{pmatrix} cos\varphi & sin\varphi \\ -sin\varphi & cos\varphi \end{pmatrix}\begin{pmatrix} x \\ y \end{pmatrix} \tag{5}$$

where x' and y' are the new coordinates after rotation which are shown in Fig. 1, thus Eq. 2 can be rewritten as,

$$\frac{\partial T}{\partial t} = k\left(\frac{\partial^2 T}{\partial x'^2} + \frac{\partial^2 T}{\partial y'^2}\right) - \|V\|\frac{\partial T}{\partial x'} \tag{6}$$

Solution to Eq. 6 above for an infinite line source, heated over time, t, was given by [7],

$$T(x', y', t) = \frac{q'}{4\pi\lambda}\int_0^t s^{-1} exp\left[\frac{-(x' - \|V\|s)^2 + y'^2}{4\kappa s}\right] ds; \quad 0 < t \tag{7}$$

where λ is the thermal conductivity ($Wm^{-1}K^{-1}$), q' is the heat input per unit length per unit time (Wm^{-1}), and t is time in seconds.

Substituting Eq. 5 into Eq.7 gives the analytical solution to Eq. 2 as,

$$T(x', y', t) = \frac{q'}{4\pi\lambda}\int_0^t s^{-1} exp\left[\frac{-(x cos\varphi + y sin\varphi - \|V\|s)^2 + (-x sin\varphi + y cos\varphi)^2}{4\kappa s}\right] ds; 0 < t \tag{8}$$

Eq. 8 is used to obtain the temperature response of each of the offset probes by substituting $\|V\|^2 = V_x^2 + V_y^2$ into Eq. 8 to give,

$$T(x', y', t) = \frac{q'}{4\pi\lambda}\int_0^t s^{-1} exp\left[\frac{-(x - V_x s)^2 + (y - V_y s)^2}{4\kappa s}\right] ds; 0 < t \tag{9}$$

However, prior to determining the flow parameters shown in the derivation from equations 2 through 9, the thermal conductivity (λ) and the thermal diffusivity (α) were each computed using equations (10) and (11) respectively.

$$\Delta T = \frac{q}{4\pi\lambda}\ln(t) \tag{10}$$

$$\Delta T = \frac{-q}{4\pi\lambda} Ei\left(\frac{-r^2}{4\alpha t}\right) \tag{11}$$

where r is the offset distance (m), q is the power input per unit length (Wm^{-1}) and Ei is the exponential integral expressed as,

$$Ei(x) = \int_{-\infty}^{x}\frac{e^{-t}}{t}dt = \gamma + \ln(x) + n = \sum_{n=1}^{\infty}\frac{x^n}{nn!} \tag{12}$$

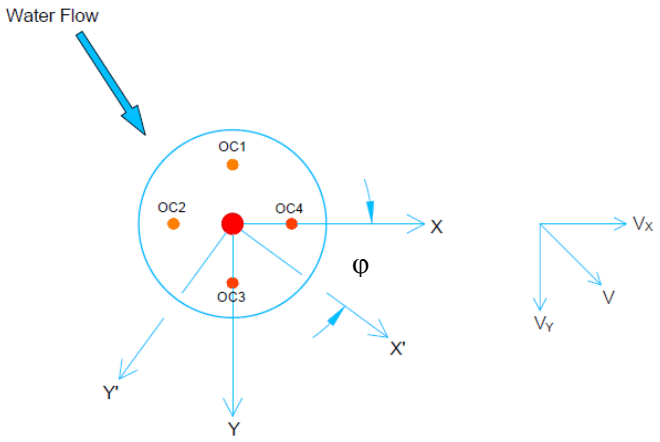

Figure 1 - Probe coordinate system (X,Y) and rotated flow coordinate system (X',Y') related by the angle, φ.

Table 1 - Coordinates of the four offset probes at a plane where r_1 through r_4 are the surface-to-center spacing between the heater and the offset probes.

Offset probes	Location at plane	
	x-coordinate	y-coordinate
OC1	0	r_1=-5.15mm
OC2	r_2=-4.90mm	0
OC3	0	r_3=5.26mm
OC4	r_4=5.13mm	0

CHAPTER 5

MATERIALS AND METHODS

The theory assumes that the soil around the SPI probe is homogeneous and isotropic and that the contact resistance between the porous media and the probes needles is negligible. Moreover, it is assumed that the offset probes have an infinitely small heat capacity and large thermal conductivity, so that the temperature measurements are instantaneous. The average distance between the centers of the heater and offset probes is about 6.90 mm, whereas the outside diameters of the offset probes are 2.44 mm and that of the heater (center probe) is 6.25 mm. The center and the offset probes were each built from stainless steel tubing, thermal epoxy, thermocouple (TC) wire, rubber stopper and nichrome heating wire which was only used in the construction of the center probe . Figure 2 below shows a well dimensioned basic structure of the SPI probe. Figure 3 shows the physical dimensions of the simulated two dimensional porous media domain with the SPI probe. The SPI probe extends perpendicularly to the illustrated (x-y) plane of the porous media domain, so that the center and the offset probes are represented by their cross-sectional circular planes within the vertical plane.

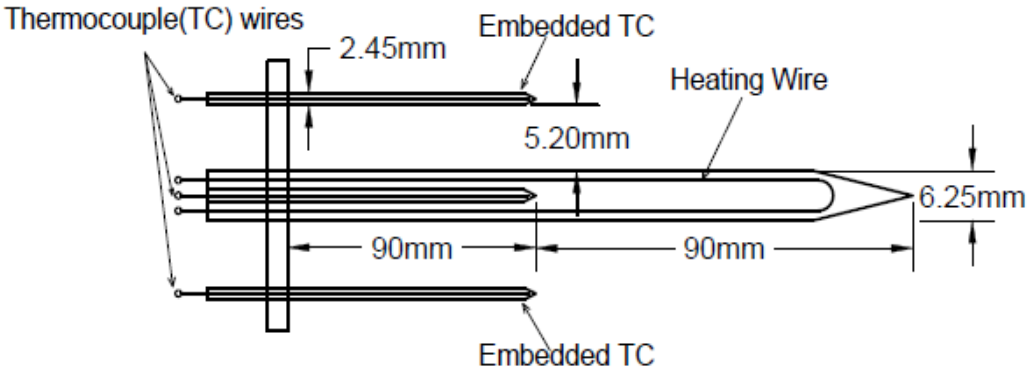

Figure 2 - A well-dimensioned basic structure of the SPI probe showing the lengths and diameters of the offset and center probes as well as the surface-to-surface distance between the center and the offset probes.

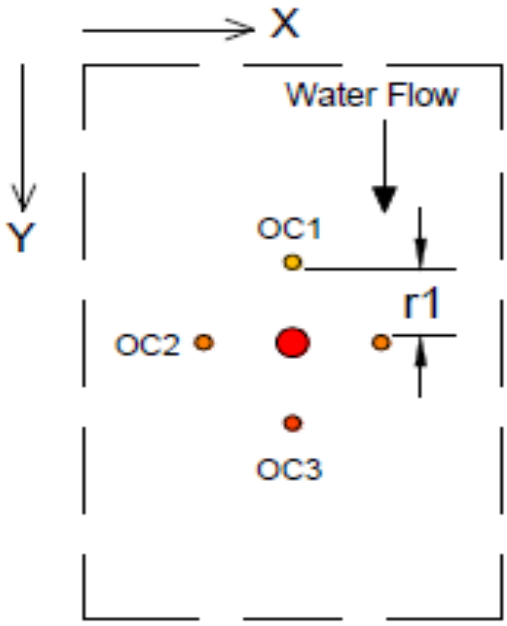

Figure 3 - The figure above shows a simulated soil domain showing the front view of the center and the offset probes with the water flow direction shown downwards.

CHAPTER 6

EXPERIMENAL SETUP

Two separate experimental setups were used to fulfill the research objective. One was for a no-flow arrangement for static tests and the other was for an arrangement of flow for flow tests. The two setups are comprised of same components. The only difference is in the elevation of the flow regulators.

For the no-flow experimental setup, the two flow regulators in the setup are both elevated to the same height.

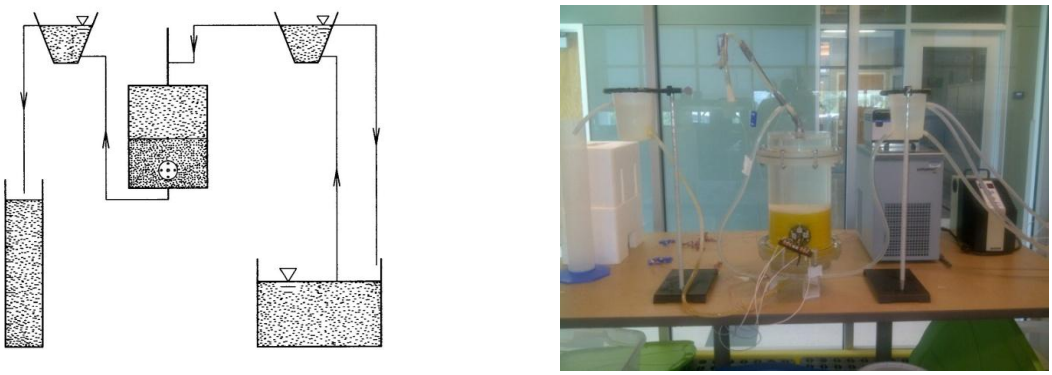

Figure 4 - Schematic and photograph the no-flow (static) experimental setup with the flow regulators elevated to the same height.

In the case of the flow experimental setup, the upstream flow regulator is maintained at a higher elevation with respect to the downstream flow regulator. This ensures that the flow through the flow cell is gravity-driven at all times. A submersible fountain water pump is used to feed degassed water to the upstream flow regulator establishing a condition of flow in the flow cell. The velocity of the water through the flow cell is varied using the white styrofoam shown in the picture below as well as an adjustable screw that keeps the ring holding the flow regulators (buckets) in place.

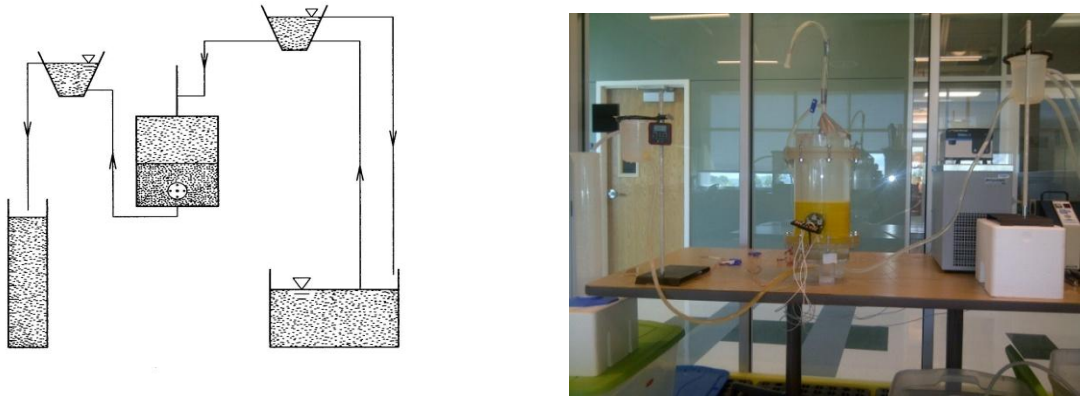

Figure 5 - Schematic and photograph the flow experimental setup with an elevation difference between upstream and downstream flow regulators.

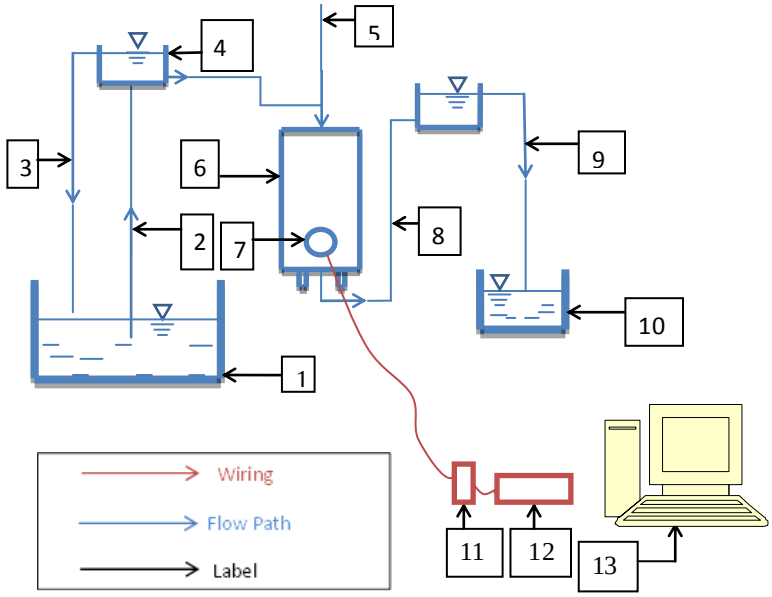

Figure 6 - Experimental setup with legend

SYSTEM COMPONENTS

1. Water reservoir
2. Intake line from reservoir
3. Return from flow regulator
4. Flow regulator
5. Bubble trap
6. Flow cell
7. SPI probe
8. Return from flow cell
9. Return line to sink
10. Graduated measuring cylinder
11. Constant-current supply unit
12. Data acquisition device
13. Computer / live monitoring system

Figure 7 - Photograph of the laboratory system

6.1 Experimental setup components and their functions

6.1.1 Storage tanks

These are plastic tanks, each of volumetric storage capacity, 109.8 L. The tanks are filled with water and left overnight to degas and reach a steady temperature. Degassing the water is necessary to eliminate bubble formation during a flow test. This gives more consistent results as opposed to when bubbles form within the system.

Figure 8 - Photograph of the storage tank used for storing water for running both static and flow tests.

6.1.2 Pump

The 120V 60Hz 0.35A submersible fountain water pump provides a constant water supply to the upstream flow regulator ensuring constant volume flow rate through the flow cell during a flow test. The pump is also used to fill up the storage tanks with water and left overnight to degas before being used for both flow and static tests.

Figure 9 - Photograph of the submersible water pump.

6.1.3 Flow cell

The flow cell contains a sieve to hold the porous media. Water is gravity-driven through the cell and the media. A sealed opening allows for the SPI probe to be inserted into the media. The flow cell is kept water and air-tight by means of o-ring seals and bolts. It is made from a transparent insulating material which allows for easy viewing of the activities taking place within it before, during and after a test. The effective volume of the flow cell is about 0.009775 m^3.

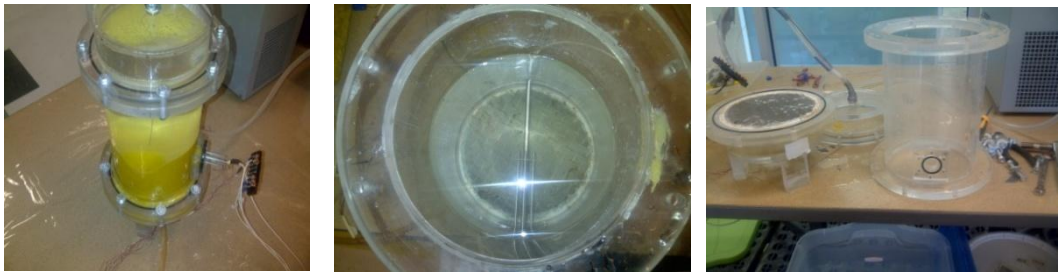

Figure 10 - Photograph of the side view (left), uncovered aerial view (center) and the individual components (right) of the flow cell.

6.1.4 Bubble trap

This is the tubing section on top of the flow cell that ensures bubble removal from the path of the flow. It is made from a 0.5588 m long, ½ inch diameter tube and fitted vertically to the top of the flow cell. It also serves as a passage for the upstream TC to read the porous media's temperature away from the probe.

Figure 11 - Photograph of the bubble trap

6.1.5 Flow regulators

The volumetric flow rate of the water through the flow cell is controlled by two open, elevated tanks. These are made from two 800mL plastic cylinders. Each tank has a spill way leading back into the storage tanks or into the sink. During a static test, the free-standing surfaces

of the water inside these flow regulators are each set to the same height to prevent any flow from occurring within the flow cell. However, during a flow test, the two flow regulators are separated by a distance using an adjustable screw along that vertical rod which serves as the main support for the flow regulators.

Figure 12 - Photograph of the downstream (left) and upstream (right) flow regulators

6.1.6 Large and small SPI's

These are each made up a center (heater) probe, four offset TCs and one upstream TC. The center probe contains a TC which is supplied with a constant current source of 3A during an actual test. The heat dissipated from the center probe is picked up as signals from the offset TCs and from the TC embedded in the center probe. From the temperature response curves obtained from these TCs, the desired thermal properties are computed. The upstream probe determines the water temperature away from the probe which ensures that both the water inside the flow cell and the storage bins are all at the same temperature prior to starting any flow test. This steady state of the system is necessary as a temperature change of 1°C over 30 minutes can negatively affect the test results.

Figure 13 - Photograph of multiple views of the SPI with the offset probes held fixed using a plastic plate

6.1.7 Graduated measuring cylinder

This is used during flow tests to measure the actual volumetric flow rate through the flow cell and from which the porous flow velocity through the flow cell is determined. Recording approximately the same time for 3-4 consecutive times that the water takes to fill up to the 2000mL mark on the graduated measuring cylinder is an indication that the flow through the flow cell is constant. At this time, a flow test is ready to be started. The measured porous flow velocity as determined by the SPI during a flow test is then compared with the actual computed flow velocity.

Figure 14 - Photograph of the 2000mL graduated measuring cylinder

6.1.8 Agilent data acquisition device

The agilent 34970A is used as a data acquisition device with a 34901A 20-channel multiplexer card. The 34901A was selected as it does not require a shunt calibration for TCs. The data acquisition device allows online monitoring of the offset and center probes during either a static or a flow test. This live monitoring is necessary for ensuring a steady state system is achieved prior to starting an actual test.

Figure 15 - Photograph of the data acquisition device

6.1.9 Power supply unit

The constant-current power supply unit supplies the heating wire embedded in the center probe with 3A of constant current. Higher power results in a better signal-to-noise ratio, but the portion of the heating wire extended outside the flow cell tends to burn above a constant current of 3A. Due to this, all static and flow test were performed with a constant current of 3A.

Figure 16 - Photograph of the constant-current power supply unit

6.2 The two orientations of the SPI probe

For testing the SPI in the lab, two orientations were considered which are 90° and 120° respectively as shown below:

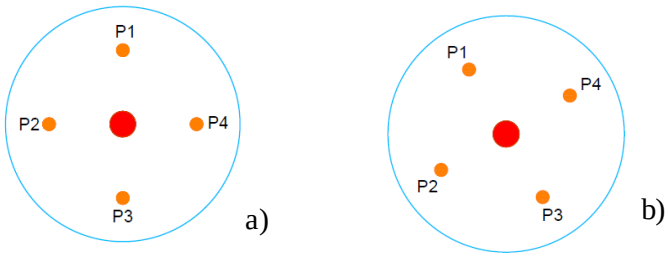

Figure 17 - a) Diagram of probe in 90-degree orientation, and of the b) 120-degree orientations. The flow is vertical and downward.

6.3 Inserting the SPI probe into the porous media

The instrument (SPI) is first mounted onto the flow cell using six screws. The flow cell is then filled with degassed water to about half the height of the flow cell and then the porous media is sprinkled around it in order to minimize the effect of the weight of the porous media on the instrument. After all the porous media has been deposited into the flow cell such that the instrument is covered entirely by the porous media, the flow cell is then covered with its lid and the remaining volume is then filled with degassed water. While filling up the flow cell, bubbles are eliminated from the system concurrently by capping and uncapping the bubble trap intermittently.


a)

b)

Figure 18 - Photograph showing the a) 120-degree and b) 90-degree orientations of the actual SPI probe when inserted into the porous media.

6.4 The live monitoring system of the experimental process

The live monitoring process is done with a desktop computer. This process helps ensure that the temperature in the saturated porous media system is uniform before the start of any experiment. Temperatures are monitored upstream the SPI probe, within the center probe, and at the downstream offset TC. When the temperature difference between upstream and downstream is approximately zero, the entire system has reached a steady temperature, and a test can be started by supplying a 3A constant-current to the center probe for a time period of 30 minutes.

During a test the live monitoring displays the temperature response of each TC ensuring that their temperatures climb steadily. This steady growth verifies that the temperature responses were not affected externally during the actual test.


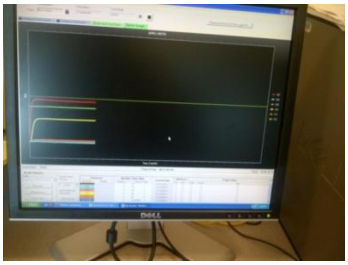

Figure 19 - Photograph of the live monitoring unit showing the temperature responses of the offset and heater probes just before (left) and during (right) an actual test.

6.5 Data processing

Processing the data retrieved from the agilent data acquisition unit via the desktop computer is a two-stage process. The data is first processed with Microsoft Excel and saved as a .txt file. This .txt file is then imported to Mathlab where the conductivity is calculated by creating a line of best fit through the log-linear region. Nonlinear curve-fitting is required to fit the diffusivity and flow vector.

6.5.1 The static case

The raw data is imported into Matlab, and the constant-current of 3A is entered in the Mathlab command window. A custom function called "Static_Grapher" is used to plot the temperature-time response from the TC inside the center probe. From the plot, two time points are selected, which outlines the log-linear region (the conductivity is most sensitive to this region).

To compute for the bulk thermal conductivity value, a second custom function called "Static_Analyzer" is used. This function takes evenly log-spaced sample points within the log-linear region, and computes a line of best fit through them. The bulk thermal conductivity is proportional to the slope of this line. The measured bulk thermal conductivity is quite sensitive to the times selected which frame the log-linear region.

The second step of static computing is to obtain the bulk thermal diffusivity. Similar to the "Static_Grapher" code, "Static_OC_Grapher" plots the temperature responses from the four (4) offset TCs. These four responses should be nearly identical when there is no flow. The "Static_OC_Analyzer" then computes the bulk thermal diffusivity for each of the four offset responses by means of nonlinear regression. The average of the four values is reported as the porous media's saturated bulk thermal diffusivity. Each of the four values may vary slightly due to the porous media inhomogeneities, and each value is dependent on the individual spacing of

the offset TCs. The equation used in the regression contains conductivity, which makes the bulk thermal diffusivity sensitive to the two time points selected as well.

6.5.2 The flow case

The bulk thermal conductivity and the bulk thermal diffusivity values computed in the static case are programmed into the flow solver by manually entering their values into the Matlab code as well as the new data file containing the temperature responses during flow. The distances of the offset TCs from the center probe need to be entered into the solver before any processing begins. These offset distances do not vary between flow tests since they have been held in a fixed position by a plastic plate. Values of these offset distances are given in Table 1.

After entering in the constant current and rotation angle of the SPI probe, the offset TC temperature responses are again plotted. The flow magnitude and angle are then fitted nonlinearly using "Flow_SV". The " Flow _SV" function first approximates a flow magnitude using the most downstream (highest response) TC, then approximates an angle using a numerical gradient, and finally it solves for the flow by fitting all four offset TC responses simultaneously with the two approximations as initial guesses. The solution usually takes between 3-5 minutes. A fitting plot is recorded as a .jpg for residual future reference.

With this Flow_SV solver, the results may be affected by a single TC. This is due to the curve fitting simultaneously fitting all four offset TCs. Thus if one has great error, particularly the downstream and hottest TC, then the flow magnitude and angle will be biased to accommodate the curve fitting of that particular response.

CHAPTER 7

EXPERIMENTAL RESULTS AND DISCUSSION

7.1 Static results

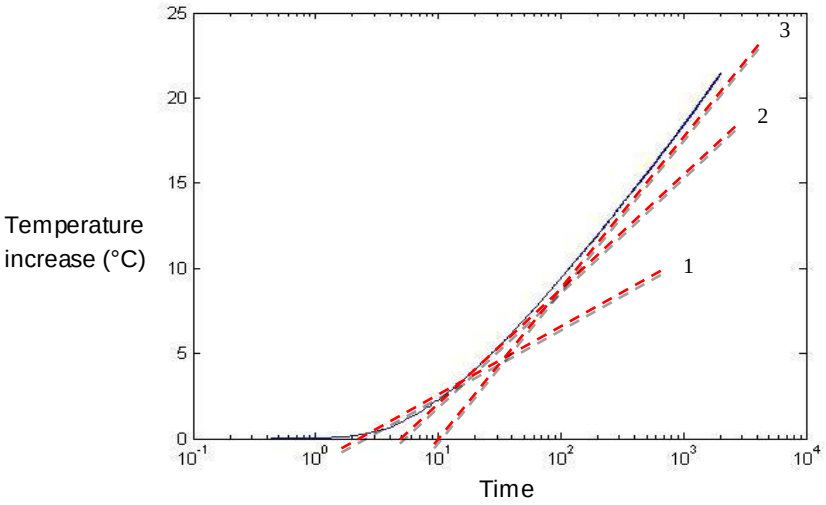

Figure 20 – Conductivity measurement sensitivity. The temperature response curve shows three possible slopes used to calculate the bulk thermal conductivity.

Bulk thermal conductivity is proportional to the slope of the log-linear region. Two points are typically selected to identify the slope. Figure 20 shows that the response never goes completely log-linear. Depending on where the two points are selected, resulting slopes may vary. It is suggested that a material's static response be observed, and two standard times picked out to calculate the slope for all subsequent tests using that material.

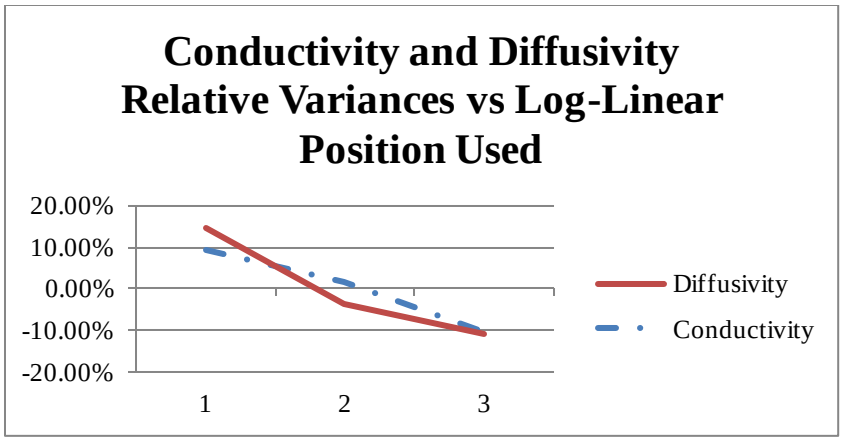

Figure 21 – Effect of varying slopes used to calculate thermal conductivity. Both the conductivity and diffusivity are calculated using the slope of the log-linear region.

Figure 21 shows how the varying slopes affect the measured values of bulk thermal conductivity and bulk thermal diffusivity. If a non-standardized selection is used, the corresponding measured thermal properties may vary as much as 15%.

7.1.1 Summary of static tests results

The static bulk thermal properties are affected by the selection of the log-linear region. To reduce this effect, we choose to select consistent times of 1000s and 1500s. The first time must be late enough to escape the initial transient region, and the second is selected using advice from B.W. Jones' work to avoid effects from the infinite media assumption.

The variation of the bulk thermal diffusivity measurements across the offset TCs has been corrected by using a thin plastic plate to hold the offset TCs in the right place thereby ensuring the same offset distances for each of the offset probes after each test run. The use of this plate has made the offset distances consistent enough to use an effective radii to account for the probe diameter's contribution to the overall radii.

7.2 Flow results

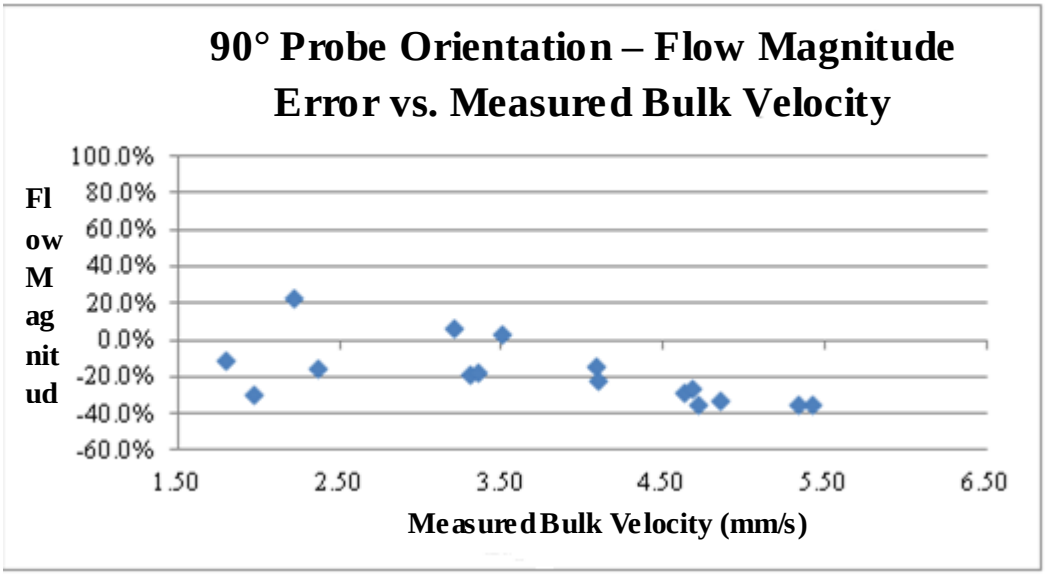

Figure 22 – Flow magnitude measurement error for increasing flow given a probe rotation of 90°. The overall trend is linear and converges to less variability with higher flow.

A trend can be seen from Fig. 22. The measured flow under-predicts the actual flow magnitude for higher flow rates. The measurement may under-predict as much as 40%, however, the overall trend is linear, and a correction factor can easily be developed. Note that this pattern exists when the probe angle is 90°. Another interesting thing to note, is that the variability of the flow measurement decreases as the flow accelerates.

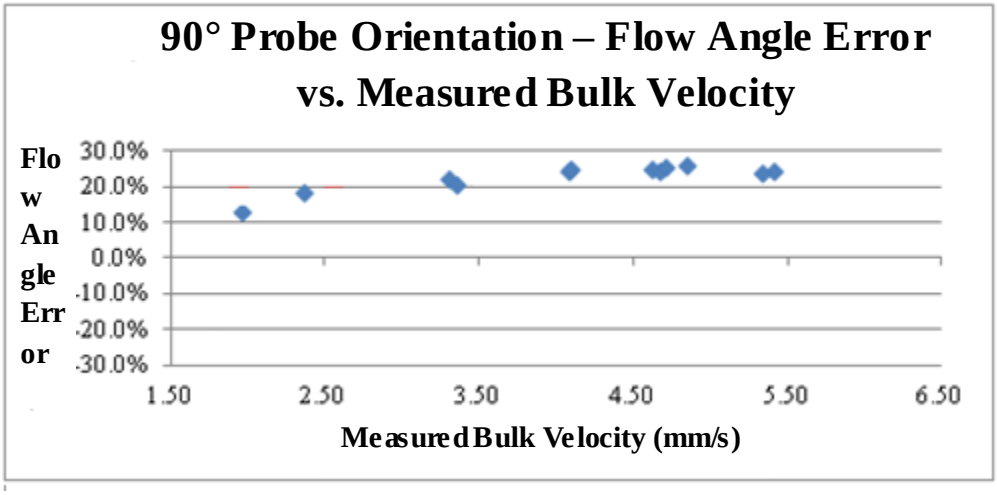

Figure 23 – Flow angle measurement error for increasing flow given a probe rotation of 90°. The error is consistently near 22% high.

Figure 23 gives the corresponding flow angle measurement error. The flow angle follows a different trend than the flow magnitude error. It is consistently high by roughly 20%, and shows very little change with respect to flow velocity. Again, a calibration can be easily determined from the data.

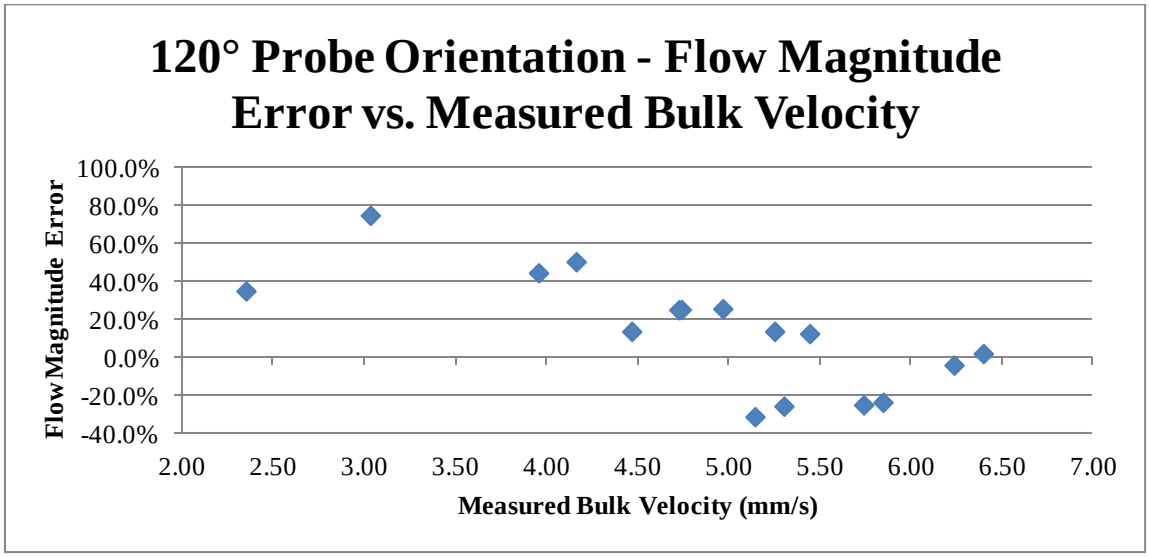

Figure 24 – Flow magnitude measurement error for increasing flow given a probe angle of 120°. An overall linear trend appears similar to the 90° orientation (Fig. 22).

Figure 24 gives the flow magnitude measurement error for increasing flow, just as Fig. 22. However, now the probe is in a different orientation, and does not have an off-set TC directly downstream. The effect on the flow magnitude measurement can be seen by greater variability, and a steeper slope as the flow increases.

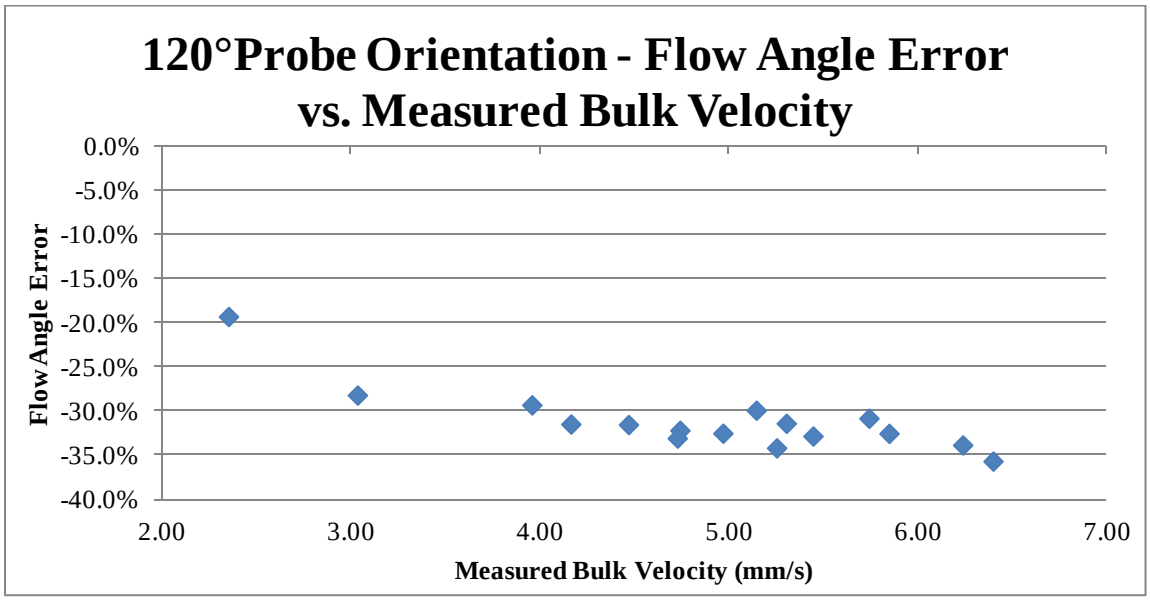

Figure 25 - Flow angle measurement error for increasing flow given a 120° probe angle. The lower flow rates exhibit less certainty, and the faster flow rates all under-predict the angle by approximately 30%.

Comparison of Fig. 25 with Fig. 23 shows a rather dramatic jump from over-predicting the angle to under predicting the angle. This could be due to the center probe's effect on the porous flow. When the diameter is large, porous flow has to curve around the probe diameter, and the off-set TCs experience a different response. The rotation of these off-set TCs inside the disrupted flow requires a calibration curve as a function of the flow angle.

While the thermal probe theory assumes a uniform flow field, Fig. 26 demonstrates that a porous flow field around a cylinder is clearly not uniform:

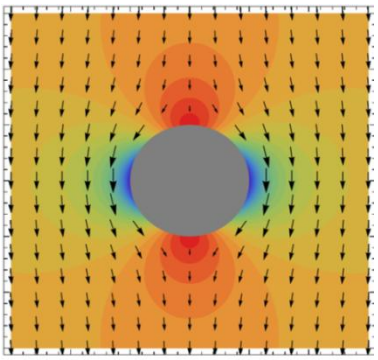

Figure 26 - Obstructed Darcy (porous media) flow. The changing flow velocity affects the temperature responses of the off-set TCs.

7.2.1 Summary of flow tests results

As made evident by the changing trends during flow tests of different orientations, the obstructed flow path must be accounted for. This disrupted flow may be solved for using Darcy's law (Eq. 1), resulting in a vector field shown in Fig. 26. Obstructed flow altered the responses of the off-set TCs enough to cause the flow angle measurement error to jump from 22% over-predicting to 30% under-predicting when the probe angle was rotated from 90° to 120°.

This change in the velocity vector may be used in Eq. (2) to stabilize the Matlab solvers.

CHAPTER 8

SUMMARY AND CONCLUSIONS

Prior to this work, no large-diameter thermal flow probe was documented. Such a probe has great implications for stream bed thermal properties, which are key to creating accurate stream bed heat models.

The keynotes of this research can therefore be summarized as:

- A large-diameter thermal flow probe (SPI) was designed, built and the functionality of the probe was determined under static and flow conditions.
- The SPI probe can be calibrated to measure the bulk thermal conductivity and bulk thermal diffusivity of any porous media.
- A flow cell was built to test the probe's ability to measure 2D porous flow.
- A plastic plate was used to secure the off-set TC, as the flexibility of the off-set TCs cause inconsistent measurement error in porous flow.

The main conclusions of this report are as follows:

- It was discovered that as high as a 15% thermal property measurement error can occur if a standard is not used in selecting the times that defines the log-linear region.
- Flow magnitude error followed a linear relationship with porous flow rate, sloping from no error at slow flow rates to under-predicting by 20% for a probe rotation of 90°. Flow magnitude error in that rotation was consistently high at approximately 22%
- The flow magnitude measurement error sloped more drastically from 50% over to 20% under with slow flow rates being too uncertain for a probe rotation of 120°. This change in the measurement error when rotating the probe is likely due to the flow interference of the off-set needles.

Future studies of large-diameter porous flow probes may include variations of porous flow properties, as well as a more comprehensive investigation of flow measurement error as a function of probe rotation. Future probe designs should attempt to address the issue of off-set needle movement during insertion.

REFERENCES

1. "Standard Test Method for Determination of Thermal Conductivity of Soil and Soft Rock by Thermal Needle Probe Procedure," ASTM D5334-08, American Society for Testing and Materials, 2008.

2. Yang, C., S.B. Jones, and G.J. Kluitenberg (2008), Penta-needle Heat Pulse Probe for Planar Vector Determination of Soil Water Flux from Optimized Thermal Parameters, Submitted for: *Water Resources Research*.

3. Hanson, J.L., Neuhaeuser, S., Yesiller, N. (2004), Development and Calibration of a Large-Scale Thermal Conductivity Probe, *Geotechnical Testing Journal*, Vol. 27, No. 4.

4. de Monte, F. (2002), An Analytical Approach to the Unsteady Heat Conduction Processes in One-dimensional Composite Media, *International Journal of Heat and Mass Transfer*, 45, 1333-1343

5. de Vries, D.A., Peck, A.J. (1958), On the Cylindrical Probe Method of Measuring Thermal Conductivity with Special Reference to Soils, *Australian Journal of Physics*, 11, 255D.

6. Jones, B.W. (1988), Thermal Conductivity Probe: Development of Method and Application to a Coarse Granular Medium, *Journal of Physics E: Scientific Instruments*, 21, 832-839.

7. Ren, T., G. J. Kluitenberg, and R. Horton (2000), Determining Soil Water Flux and Pore Water Velocity by a Heat Pulse Technique, *Soil Sci. Soc. Am J*, 64(2), 552-560.

8. Bristow, K. L., G. J. Kluittenberg and R. Horton (1994), Measurement of soil thermal properties with a dual-probe heat pulse technique, *Soil Sci. Soc. Am. J.*, 58, 1288-1294.

9. Bristow, K. L.(1998), Measurement of thermal properties and water content of unsaturated sandy soil using dual-probe heat-pulse probes, *Agric. For. Meterorol.* , 89, 75-84.

10. Hammerschmidt, U. & Sabuga,W., (2000), Transient Hot Wire Method (THW) method: Uncertainty assessment, *Int. J. Thermophysics*, 21,pp. 1255-1278. Carslaw, H.S. Jaeger, J. C.(1946) *Conduction of Heat in Solids*, 2nd Edition, Oxford University Press, New York.

11. De Groot, J.J., Kestin, J. & Sookiazian, H., (1974), Instrument to measure the thermal conductivity of gases, *Physica*, 75,pp. 454-482.

12. Healy, J.J., de Groot, J.J. & Kestin, J., (1976), The theory of the Transient Hot-Wire method for measuring thermal conductivity, *Physica*, 82C, pp. 392-408.

13. Kestin, J., & Wakeham, W.A., (1978), A contribution to the theory of the transient hot-wire technique for thermal conductivity measurements", *Physica*, 92A, pp. 102-116.

14. J. H. Blackwell, (1954), A transient flow method for determination of thermal constants of insulating materials in bulk, *Journal of Applied Physics*, Vol 25,No.2.

15. Schneider, P.J. (1955), *Conduction Heat Transfer*, Addison-Wesley, Reading, Massachusetts.